GA–A26224

DRIFT-KINETIC SIMULATIONS OF NEOCLASSICAL TRANSPORT

by
E.A. BELLI and J. CANDY

AUGUST 2008

GENERAL ATOMICS

GA– A26224

DRIFT-KINETIC SIMULATIONS OF NEOCLASSICAL TRANSPORT

by
E.A. BELLI and J. CANDY

This is a preprint of a paper to be presented at the Theory of Fusion Plasmas, Joint Varenna-Lausanne International Workshop, August 25-29, 2008, in Varenna, Italy, and to be published in the *Proceedings*.

Work supported by
the U.S. Department of Energy
under DE-FG02-95ER54309

GENERAL ATOMICS PROJECT 03726
AUGUST 2008

Drift-Kinetic Simulations of Neoclassical Transport

E.A. Belli and J. Candy

General Atomics, P.O. Box 85608, San Diego, CA 92186-5608, USA

Abstract. We present results from numerical studies of neoclassical transport for multi-species plasmas. The code, NEO, provides a first-principles based calculation of the neoclassical transport coefficients directly from solution of the distribution function by solving a hierarchy of equations derived by expanding the fundamental drift-kinetic equation in powers of ρ_{*i}, the ratio of the ion gyroradius to system size. It extends previous studies by including the self-consistent coupling of electrons and multiple ion species and strong toroidal rotation effects. Systematic calculations of the second-order particle and energy fluxes and first-order plasma flows and bootstrap current and comparisons with existing theories are given for multi-species plasmas. The ambipolar relation $\sum_a z_a \Gamma_a = 0$, which can only be maintained with complete cross-species collisional coupling, is confirmed. The effects of plasma shaping are also explored.

Keywords: neoclassical, transport, simulation
PACS: 52.25.Dg,52.25.Fi, 52.65.-y

1. INTRODUCTION

Accurate simulation of turbulence and transport in tokamak edge plasmas requires a full-f kinetic formulation in which equilibrium and fluctuation-scale dynamics are merged. While neoclassical transport is generally subdominant to anomalous transport by at least one order of magnitude in the core, neoclassical dynamics is believed to be important in explaining enhanced edge confinement phenomena, such as the formation of transport barriers in the H-mode edge due to $E \times B$ shear stabilization [1]. Thus, kinetic simulations incorporating such effects are of interest.

For this purpose, we have developed a new code NEO, which provides a direct numerical solution of the drift-kinetic equation (DKE) based on the drift-kinetic operator of Hazeltine [2], including coupling to the Poisson equation. While analytic estimates for neoclassical transport coefficients were first developed in the 1970s, they were based on a hierarchy of approximations, such as simplified geometry, limited collisionality regimes, small electron-to-ion mass ratio, etc. (For more details, see the review articles by Hinton and Hazeltine [3] and Hirshman and Sigmar [4].) Later extensions include the well-known Chang-Hinton formula for the ion energy flux [5], which allows for experimentally relevant values of collisionality and aspect ratio for circular plasmas, the analysis of Hirshman et al. [6, 7], which studies the transport of impurities, and extensions of the drift-kinetic formulation to include strong rotation effects by Hinton and Wong [8] and Catto et al. [9]. However, none of the analytic formulae can accurately treat plasma shaping or self-consistent interspecies coupling over all collisionality regimes. While some improvement over the analytic formulae is possible with the NCLASS code [10], which is itself based on a combination of moment methods and analytic formulae for circular plasmas, the correspondance of NCLASS results to direct solution of the DKE has not been established. Our approach improves on existing calculations by solving a hierarchy of equations derived using the traditional expansion procedure in powers of ρ_{*i}, the ratio of the ion gyroradius to system size, and thus represents a first-principles approach. Our final result is in some sense an exact solution for the standard second-order neoclassical fluxes unrestricted by orderings in aspect ratio, collision frequency, etc.

In this paper, we summarize NEO simulation results of neoclassical transport for multi-species plasmas. A more detailed account of results in the diamagnetic ordering limit appears in Ref. [11]. The remainder of this paper is organized as follows. In Sec. 2, we describe the basic simulation model and numerical methods used in NEO. In Sec. 3, the simulation results are presented, including comparisons of the second-order neoclassical fluxes and first-order bootstrap current with analytic theory. Studies of the effects of heavy impurity ions, strong toroidal rotation, and shaping are also presented. Finally, a summary of the results is given in Sec. 4.

2. NEOCLASSICAL SIMULATION MODEL

In NEO, we solve a hierarchy of equations based on expanding the fundamental drift-kinetic equation in powers of $\rho_{*i} = \rho_i/a$, the ratio of the ion gyroradius $\rho_i \doteq (c\sqrt{m_i T_{0i}})/(z_i eB)$ to the system size. Thus the distribution function for each species a is expanded as

$$f_a = f_{0a} + f_{1a} + f_{2a} + \ldots \tag{1}$$

The equations are generalized to include the effects of strong rotation based on the derivation by Hinton and Wong [8], who extended the original neoclassical theory [2], which assumes the diamagnetic ordering, to allow for the ratio of the species flow to the thermal speed to be of arbitrary size. Thus, the leading-order electric field is one order larger than in the diamagnetic drift ordering, as required to maintain the asumption of slow temporal change $\frac{\partial}{\partial t} \sim \rho_{*i}^2 \Omega_{ci}$ (where $\Omega_{ci} = z_i eB/(m_i c)$ is the cyclotron frequency) in the presence of a large perpendicular flow, i.e.

$$\Phi = \Phi_{-1} + \Phi_0 + \Phi_1 + \Phi_2 + \ldots \,. \tag{2}$$

Hinton and Wong have shown that Φ_{-1} is a flux function and that the zeroth-order flow speed must be purely toroidal and species independent: $\vec{V}_{0a} = \omega R^2 \nabla\varphi$ such that the angular rotation frequency is related to Φ_{-1} by $\omega(\psi) = -\frac{d\Phi_{-1}}{d\psi}$, where ψ, the poloidal flux divided by 2π, is the flux surface label. Here we write the equations in the rotating frame, adopting the velocity coordinates $E = v^2/2 + \lambda_a(\theta) v_{ta}^2$ and $\mu = v_\perp^2/(2B)$, where v is the rotating frame speed, $\lambda_a(\theta) \doteq (z_a e/T_{0a})\tilde{\Phi}_0(\theta) - \omega^2 R(\theta)^2/(2v_{ta}^2)$, and $\tilde{\Phi}_0(\psi,\theta)$ is the poloidally-varying part of the potential, $\tilde{\Phi}_0(\psi,\theta) = \Phi_0(\psi,\theta) - \langle\Phi_0\rangle$. The equations reduce to the usual diamagnetic ordering in the limit $\Phi_{-1} \to 0$.

2.1. Equilibrium equations

The $\mathscr{O}(1)$ equilibrium equation is

$$v_\parallel \cdot \nabla f_{0a} = C_{a,a}\left(f_{0a}, f_{0a}\right) \ . \tag{3}$$

Thus, the zeroth-order distribution function is Maxwellian in the rotating frame with the form

$$f_{0a} = \frac{n_{0a}}{(2\pi T_{0a}/m_a)^{3/2}} e^{-v^2/2v_{ta}^2} \tag{4}$$

where $v_{ta} = \sqrt{T_{0a}/m_a}$ is the thermal speed. The temperature, $T_{0a} = T_{0a}(\psi)$, is a flux function but the density, $n_{0a}(\psi,\theta) = N_{0a}(\psi)\exp(-\lambda(\theta))$, is not. The poloidal potential $\tilde{\Phi}_0(\psi,\theta)$ is determined by the $\mathscr{O}(1)$ Poisson equation, which reduces to the usual quasi-neutrality relation

$$\sum_a z_a e\, n_{0a} = 0 \ . \tag{5}$$

For a general multi-species plasma, we use Newton's method to solve for the complete equilibrium densities, given as input the values of the densities at the outboard midplane.

2.2. First-order equations

The $\mathscr{O}(\rho_{*i})$ contribution to the drift-kinetic equation is

$$\begin{aligned} v_\parallel \cdot \nabla g_{1a} - \textstyle\sum_b C_{ab}^L &= -f_{0a}\left(\tfrac{d\ln N_{0a}}{d\psi} + \tfrac{z_a e}{T_{0a}}\tfrac{d\langle\Phi_0\rangle}{d\psi}\right) v_\parallel \cdot \nabla\alpha_1 \\ &- f_{0a}\tfrac{d\ln T_{0a}}{d\psi} v_\parallel \cdot \nabla\left[\alpha_1\left(\tfrac{E}{v_{ta}^2} - \tfrac{3}{2}\right)\right] - f_{0a}\tfrac{d\ln\omega}{d\psi} v_\parallel \cdot \nabla\alpha_2 \ , \end{aligned} \tag{6}$$

where $g_{1a} = f_{1a} + f_{0a}\frac{z_a e}{T_{0a}}\Phi_1$ is the nonadiabatic distribution function, C_{ab}^L is the linearized collision operator, and the arguments of the RHS source term derivatives are given by

$$\alpha_1 = \frac{m_a c}{z_a e}\left(\frac{I v_\parallel}{B} + \omega R^2\right) \ , \quad \alpha_2 = \frac{m_a c\omega}{z_a e 2 v_{ta}^2}\left[\left(\frac{I v_\parallel}{B} + \omega R^2\right)^2 + \mu\frac{|\nabla\psi|^2}{B}\right] \ . \tag{7}$$

The first-order potential can obtained from g_{1a} via the $\mathscr{O}(\rho_{*i})$ Poisson equation

$$\sum_a \frac{z_a^2 e^2 n_{0a}}{T_{0a}}\Phi_1 = \sum_a z_a e\int d^3v\, g_{1a} \ . \tag{8}$$

The corresponding second-order neoclassical particle and energy fluxes are given by

$$\Gamma_{2a} = \left\langle \int d^3v\, v_\parallel \hat{b}\cdot\nabla\alpha_1 g_{1a}\right\rangle \ , \quad Q_{2a} = \left\langle \int d^3v\, T_{0a} v_\parallel \hat{b}\cdot\nabla\left(\alpha_1\frac{E}{v_{ta}^2} + \alpha_2\right) g_{1a}\right\rangle \ . \tag{9}$$

The first-order bootstrap current is given by

$$\left\langle j_{\parallel}B\right\rangle = \sum_a z_a e \left\langle n_{0a} U_{\parallel_{1a}} B \right\rangle \quad \text{, where} \quad U_{\parallel_{1a}} = \frac{\omega I}{B} + \frac{1}{n_{0a}} \int d^3v\, v_{\parallel} g_{1a} \,. \tag{10}$$

The numerical approach used in NEO is sketched in Ref. [11] and will be described in detail in a future publication. Briefly, we use a mixture of spectral and finite-difference approximations. We adopt the kinetic energy $\varepsilon_a = v^2/(2v_{ta}^2)$ and cosine of the pitch angle $\xi = v_{\parallel}/v$ as the velocity space coordinates, since the collision operator, described in the next section, is aligned in these coordinates. We use basis function expansions of Chebyshev polynomials in energy and Legendre polynomials in ξ. A mesh is used in the spatial variables r and θ. The resulting matrix system is solved with a standard sparse solver.

2.3. Model forms of the linearized collision operator

In this paper, we consider three model collision operators, described as follows in descending order of sophistication. The full Hirshman-Sigmar operator [12] (HS) is obtained by a sophisticated expansion and renormalization of the linearized Fokker-Planck operator. The operator conserves number, momentum, energy, is self-adjoint and has an H-theorem. It contains a pitch-angle scattering Lorentz operator and an energy diffusion term as well as models for the deceleration effect arising from dynamic friction and for heating friction effects. The zeroth-order Hirshman-Sigmar operator [6] (HS0) is a reduced form of the full Hirshman-Sigmar operator which retains just the Lorentz operator and momentum-restoring contributions. It does include, however, the distinction between the pitch-angle diffusion frequency and the slowing-down frequency, the latter of which is known to be important for accurately modeling collisions between species with similar masses and thus is essential for studies of multi-ion plasmas. Finally, for comparative purposes, we also present results for the Connor model [13], a very simple operator based on a multi-species extension of the so-called Kovrizhnikh operator [14] which is useful for analytic work. Similar to the zeroth-order Hirshman-Sigmar operator, the Connor model also contains just a pitch angle scattering term and a momentum-restoring term. However, the model does not distinguish between the deflection frequency and the slowing-down frequency and, rather, the form of the single collision frequency is made to depend asymmetrically on the relative masses of the colliding particles based on an asymptotic expansion. The Connor model is valid for Lorentz plasmas, such as pure plasmas and multi-species plasmas containing only an additional high-z impurity.

We note that the properties of the collision model are important in determining the neoclassical physics, specifically regarding ambipolarity. It can easily be seen from the first-order kinetic equation that the plasma maintains ambipolarity $\sum_a z_a \Gamma_{2a}$ only if the general momentum conservation property collision operator $\int d^3v\, v_{\parallel} \sum_b C_{ab} g_{1b}$ is properly maintained, as is done here.

3. SIMULATION RESULTS

The results presented in this paper are based on the General Atomics standard case parameters [15]: $r/a = 0.5$ and $R_0/a = 3$ (inverse aspect ratio $\varepsilon \doteq r/R_0$ = 1/6), $q = 2$, $a/L_{ni} = a/L_{ne} = 1$, $a/L_{Ti} = a/L_{Te} = 3$, $T_{0i} = T_{0e}$. s-α geometry with $\alpha = q^2 R_0 d\beta/dr = 0$ and the diamagnetic limit ($\omega = 0$) are assumed unless otherwise specified. All cases with kinetic electrons use the true electron mass, and the main ion is always taken to be deuterium. Scans are performed over a wide range of collision frequency, $\tau_{ii}^{-1} \doteq \sqrt{2}\pi e^4 z_i^4 n_{0i} \ln\Lambda/(m_i^{1/2} T_{0i}^{3/2})$. The energy fluxes are given in units of the ion gyroBohm of energy flux, $Q_{GB} \doteq n_{0i} T_{0i} v_{ti} \rho_{0i}^2/a^2$, where $\rho_{0i} \doteq (c\sqrt{m_i T_{0i}})/(z_i e B_0)$.

3.1. Basic assessment of code validity

To establish the physical accuracy of the code results, we perform simulations for a limited test case consisting of adiabatic electrons, such that only C_{ii} is nonzero, and in the banana regime of collisionality. In these limits, the most accurate analytic result for the calculation of Q_i, given by Taguchi's theory [16], is valid. In Fig. 1, we plot the NEO numerical results against Taguchi's theory as well as theoretical predictions from Hinton and Hazeltine [3] (HH theory) and Chang and Hinton [5] (CH theory). The salient result is that the Hirshman-Sigmar collision model accurately recovers Taguchi's theory, while the zeroth-order Hirshman-Sigmar collision model and the Connor collision model both underestimate the heat flux, with the Connor model results more closely following the Hinton-Hazeltine theory. The Chang-Hinton formula, which provides finite-ε corrections to the Hinton-Hazeltine theory and is the most widely used of the theoretical models, is shown to overestimate the transport, by about 22%. Overall, these results not only verify the code but further suggest that an accurate model for ion-ion collisions, which specifically includes energy diffusion, is potentially important for modeling experiments. It is also clear from comparing the zeroth-order Hirshman-Sigmar model with the Connor model that the deceleration effect, represented by the slowing-down frequency ν^S in the Hirshman-Sigmar model, can be significant.

3.2. Results with self-consistent electron dynamics

The second-order particle and energy fluxes computed with NEO are shown in Fig. 2. Hinton-Hazeltine analytic predictions [3] are also shown. In contrast to the simulations in Fig. 1, which treated only a single ion species, the present results properly account for the exact electron-mass corrections due to C_{ie}, which are not retained in the theory. We remark that the simulations dynamically recover ambipolarity, $\Gamma_i = \Gamma_e$, accurate at this numerical resolution to about three significant figures. For this reason, we plot only Γ_i. As noted previously, ambipolarity can only be maintained with complete ion-electron collisional coupling. While the ion particle flux, which arises due to the cross-species parallel momentum exhange, varies on the electron scale, the ion energy flux is generally $O(\sqrt{m_i/m_e})$ larger than the electron energy flux. Comparing the collision

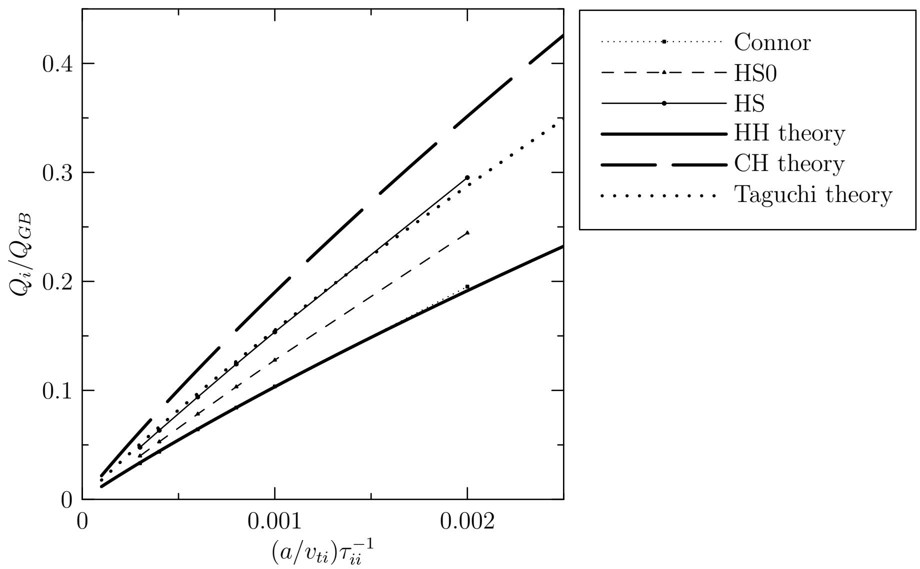

FIGURE 1. Ion particle flux versus collision rate in the banana regime for the case of adiabatic electrons. NEO results from all three collision operators are shown, along with predictions from the Hinton-Hazeltine theory (HH theory), Chang-Hinton theory (CH theory), and Taguchi theory.

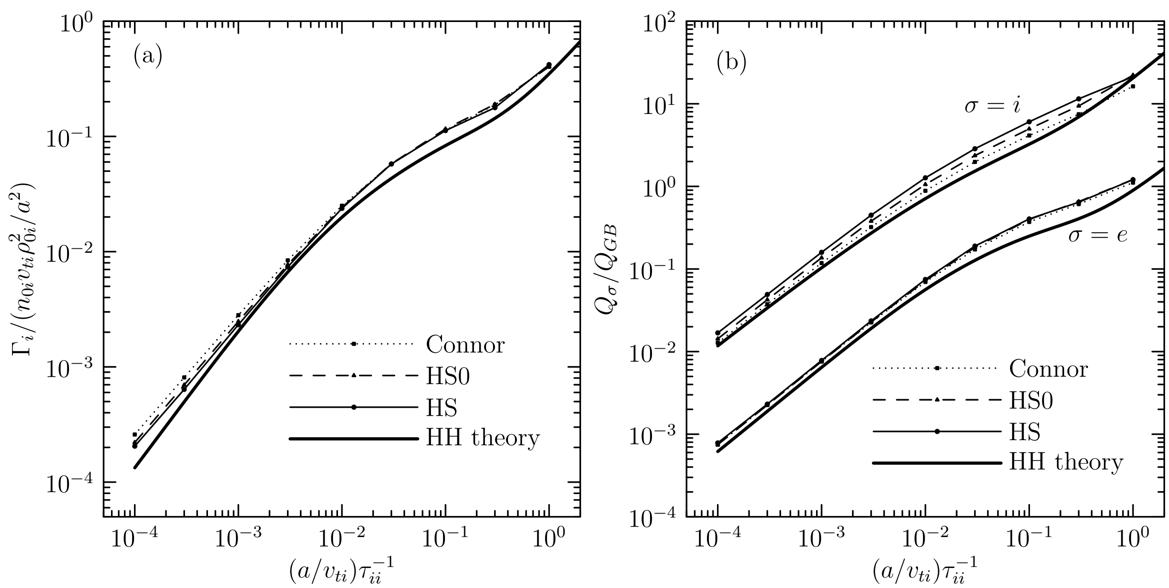

FIGURE 2. (a) Ion particle flux and (b) ion and electron energy fluxes versus collision rate. NEO results from all three collision operators are shown, along with the prediction from the Hinton-Hazeltine theory (HH theory). Since the particle flux is ambipolar to high accuracy, only the ion values are shown.

models themselves in these results, a large variation is generally not found – with the exception that the full Hirshman-Sigmar model consistently yields a larger energy flux in all collisionality regimes for both species.

In addition to the particle and energy fluxes, accurate modeling of bootstrap current

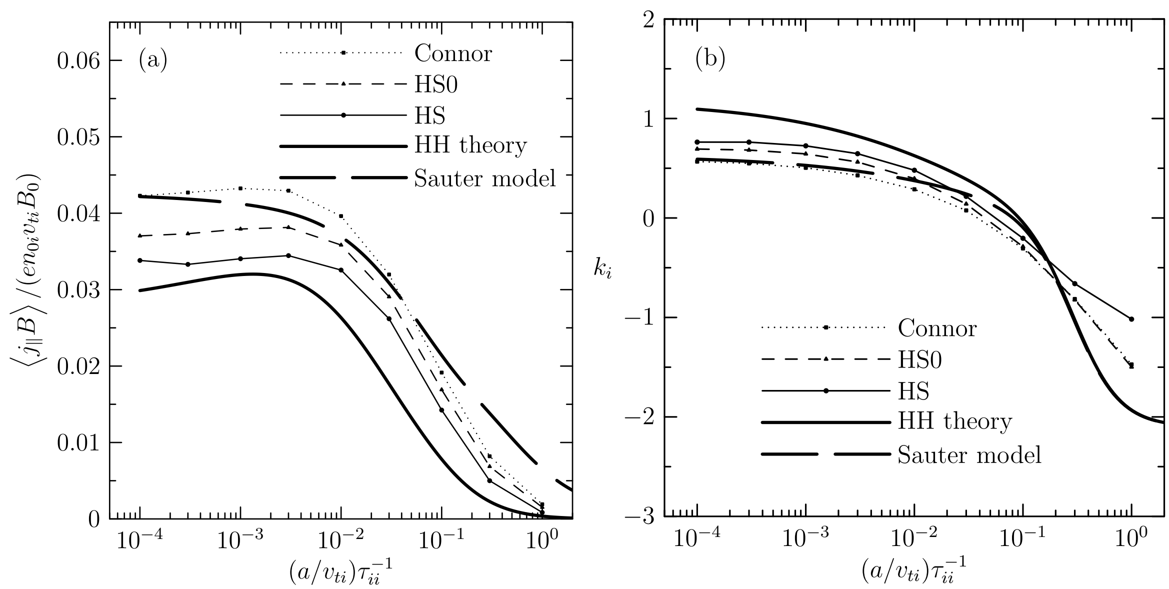

FIGURE 3. (a) Bootstrap current and (b) ion flow coefficient versus collision rate. NEO results from all three collision operators are shown, along with predictions from the Hinton-Hazeltine theory (HH theory) and the Sauter model.

is also of interest. This is shown in Fig. 3a, with the Hinton-Hazeltine theory and the fits by Sauter et al. [17] shown for comparison. The Sauter model is based on a fitting formula using the fraction of trapped particles, ν_{*i}, and z_i as parameters. It therefore includes some finite-aspect-ratio corrections which, as shown, are most significant in the banana regime. In general, we find that the NEO results for the bootstrap current lie between the two theories. Further insight can be achieved by considering the variation of the dimensionless flow coefficient k_a, defined in terms of the parallel flow by

$$\left\langle U_\parallel B \right\rangle_{1a} = \langle \hat{\omega}_a \rangle I + k_a(r) \frac{cT_{0a} I}{z_a e} \frac{d \ln T_{0a}}{d\psi} \ , \tag{11}$$

where

$$\hat{\omega}_a \doteq -\frac{cT_{0a}}{z_a e} \left[\frac{d \ln N_{0a}}{d\psi} + \frac{d \ln T_{0a}}{d\psi} (1 + \lambda_a(\theta)) + \frac{z_a e}{T_{0a}} \frac{d \langle \Phi_0 \rangle}{d\psi} + \frac{\omega R^2}{v_{ta}^2} \frac{d\omega}{d\psi} \right] . \tag{12}$$

In the limit of weak rotation, $\hat{\omega}_a$ is the usual diamagnetic frequency and Eq. (11) becomes the usual standard neoclassical relation [21]. As Sauter explains, the ion dimensionless flow coefficient k_i depends very sensitively on both ε and ν_{*i} and thus the two effects cannot be decoupled, as is usually done in the analytic theory. Unlike the other coefficients in the Sauter model, the model for k_i is based on a modification of the Harris model [18], which smoothly connects the Hirshman collisionless model and the Hinton-Hazeltine collisional model. As shown in Fig. 3b, we find with NEO that, with the full Hirshman-Sigmar model, k_i is larger than the Sauter prediction. This is consistent with the smaller bootstrap current observed in Fig. 3a.

3.3. Impurity dynamics and rotation effects

The effect of heavy-ion impurities on the ion neoclassical transport has also been studied. For these simulations, we use the standard case parameters and include fully-stripped carbon impurity ions with $z_I = 6$. The ion-carbon density ratio is specified through the impurity charge dilution factor, $f_I \doteq z_I(n_{0I}/n_{0e})$ and is taken to be $f_I = 0.1$. The impurity equilibrium temperature and temperature gradient scale length are equal to the main ion values. Scans are performed over a wide range of collision frequency, with the ion and impurity collision frequencies varied consistently, assuming that the Coulomb logarithm is species-independent.

Results are shown in Figs. 4 and 5, together with the analytic prediction of Hirshman and Sigmar [6, 7], which is based on the zeroth-order Hirshman-Sigmar collision model and interpolates to connect the banana and plateau regime theories. For the particle flux, shown in Fig. 4, all operators perform well for the electron flux, but for ion and impurity flux the Connor model performs poorly. This is due to the fact that the Connor operator does not model the deceleration effect represented by the slowing-down frequency, which is important for collisions between species with similar masses. The full and zeroth-order Hirshman-Sigmar operators agree closely except at the highest collision frequencies, where presumably energy scattering begins to dominate. For the energy flux, shown in Fig. 5, the collision models produce similar trends, although the less accurate models slightly underpredict the ion energy flux (similar to the pure plasma case shown in Fig. 2b). Comparing the NEO fluxes with the theory, we ultimately find that the Hirshman-Sigmar theory gives particle flux ratios so inaccurate as to be useless. The theory does a better job of predicting the electron and ion energy fluxes, but gives the wrong sign of the impurity energy flux at moderate to high collision frequency. These results reflect a general limitation of analytic theories for multi-species plasmas (based on collisionally-interpolative formulas) due to inadequate modeling of the multitude of accessible collisional regimes for any given τ_{ii}^{-1} considering all of the collisional species pairs. For this reason, multi-species analytic theories are typically valid only in the weak-coupling limit, and, overall, for accurate calculation of impurity transport, the Hirshman-Sigmar formulas should be avoided.

Figures 4d and 5d show the relative effect of strong toroidal rotation. Here we show the variation of the fluxes with the ion Mach number squared, $M_i^2 \doteq m_i \omega^2 R_0^2/(T_{0e}+T_{0i})$, for the case of a single collision frequency in the banana regime. Zero rotation shear is assumed. Most noticeably, the electrons are least affected by the rotation, as excepted since the influence of the centrifugal force is weak due to their small mass. The impurity fluxes are largely enhanced by the rotation, due to the increase in the effective fraction of trapped particles. Due to ambipolarity, the magnitude of the ion particle flux is also enhanced, while the ion energy flux, which is generally only weakly influenced by the collision friction with the impurities, is slightly suppressed.

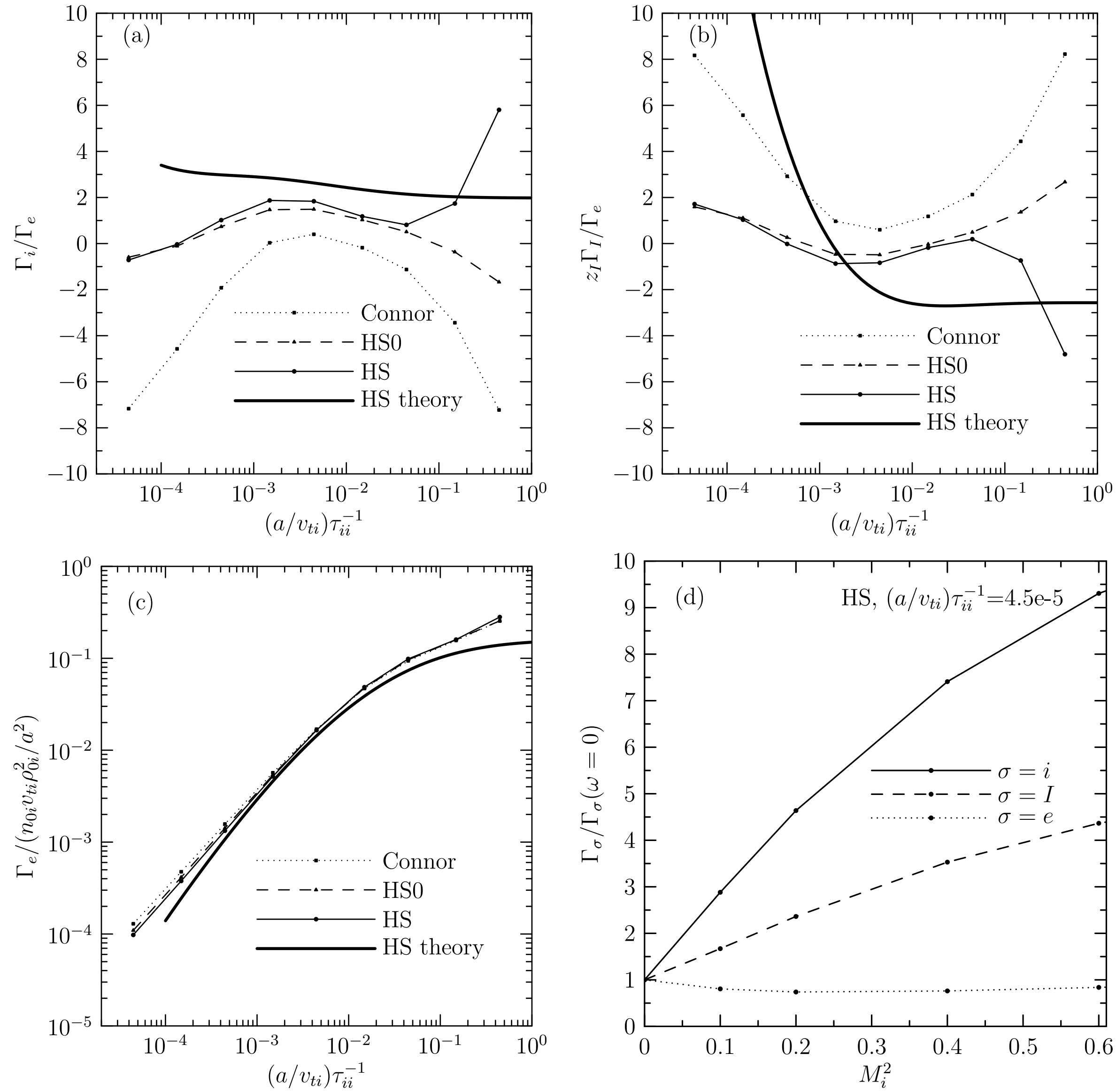

FIGURE 4. Variation of the (a) ion, (b) carbon impurity and (c) electron particle fluxes with collision frequency (for ω=0). NEO results from all three collision operators are shown, along with the prediction from the Hirshman-Sigmar interpolatory formula (HS theory). Also shown (d) is the variation of the particle fluxes with Mach number squared in the banana regime using the HS collision operator in NEO.

3.4. Plasma Shape

The effect of cross-sectional shaping on the neoclassical transport has also been studied using the Miller local equilibrium model [19]. In the simulation we assume electrons are adiabatic and use the full Hirshman-Sigmar collision operator. For these results, we generalize the definition of the normalizing gyroBohm unit of energy flux as $Q_{GB} \doteq n_{0i}T_{0i}v_{ti}\rho_{i,unit}^2/a^2$, where $\rho_{unit} \doteq (c\sqrt{m_iT_{0i}})/(z_ieB_{\text{unit}})$ is the unit gyroradius.

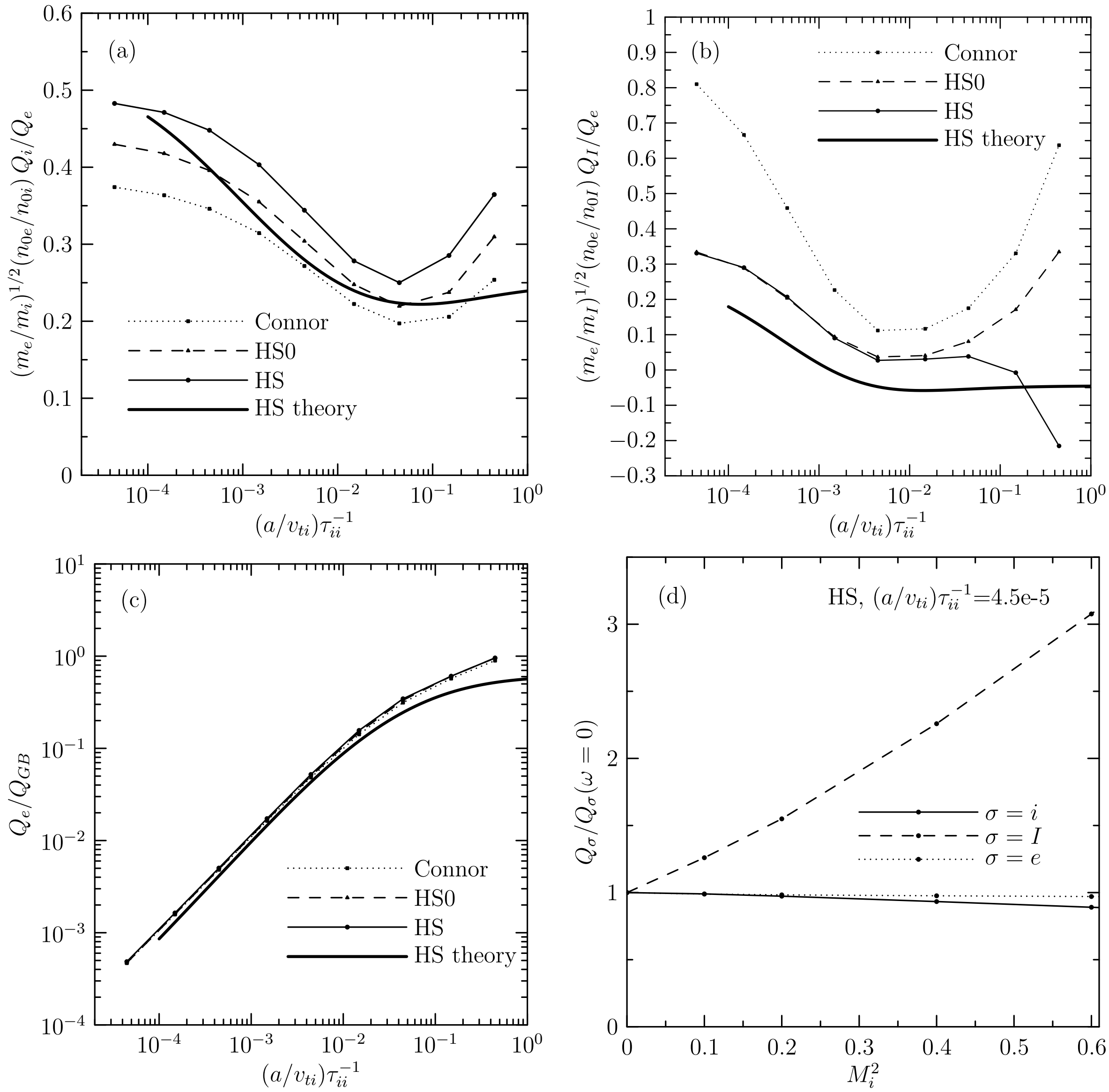

FIGURE 5. Variation of the (a) ion, (b) carbon impurity and (c) electron energy fluxes with collision frequency (for ω=0). NEO results from all three collision operators are shown, along with the prediction from the Hirshman-Sigmar interpolatory formula (HS theory). Also shown (d) is the variation of the energy fluxes with Mach number squared in the banana regime using the HS collision operator in NEO.

Here $B_{\text{unit}}(r) = (q/r)d\psi/dr$ is the effective magnetic field strength [20].

Figure 6 shows the effect of two significant shaping parameters – triangularity (δ) and elongation (κ) – on the ion energy flux. For comparison, we show both the standard Chang-Hinton (CH theory) results for the ion energy flux, as well as a modified formula (M-CH formula) which evaluates the magnetic field averages using the Miller $B(\theta)$ rather than the explicit analytic form. This modification accounts for the lesser effect of shaping which is to modify the geometrical factors which appear in the kinetic equation.

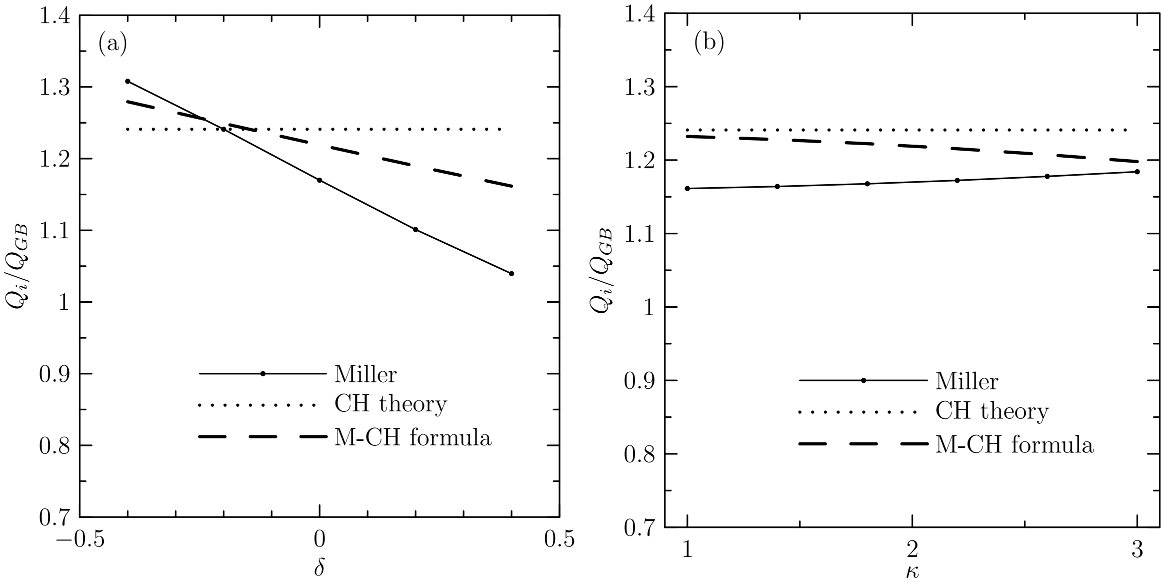

FIGURE 6. Ion energy flux as a function of (a) triangularity and (b) elongation using the Miller geometry model in NEO. Electrons are adiabatic, and the HS collision operator is used. Also shown are the Chang-Hinton theory (CH theory) and modified Chang-Hinton formula (M-CH formula).

The primary effect of shaping is to modify B_{unit} from the on-axis value, e.g. the dominant B_{unit} scaling is generally $B_{unit} \sim \kappa B_0$. Thus, it is crucial that the analytic formulas account for this overall shift in the effective magnetic field strength. This is done via evaluation of the gyroradius using B_{unit}, and not the on-axis field, in both the standard and the modified formulas. Here we are interested in comparing only the qualitative trends of NEO and M-CH with shaping, as we have previously established in Sec. 3.1 that the Chang-Hinton model overestimates the ion energy flux. In the case of κ and δ, there is explicit parameteric only in the M-CH model. Here, the model is correct in the case of δ, as shown in Fig. 6a, but gives the wrong trend for κ, as shown in Fig. 6b. This result suggests that the use of the exact magnetic field in the Chang-Hinton formula does not accurately model the scaling with shaping.

4. SUMMARY

A new Eulerian code, NEO, has been developed for numerical studies of neoclassical transport. NEO solves a hierarchy of equations derived by expanding the DKE in powers of ρ_{*i} and thus represents a first-principles calculation of the neoclassical transport coefficients for general plasma shape. NEO extends previous numerical studies by including the self-consistent coupling of electrons and multiple ion species and strong toroidal rotation.

For benchmarking, comparisons of the second-order transport coefficients with various analytic theories have been presented. Three model collision operators were compared: the full Hirshman-Sigmar operator, the zeroth-order Hirshman-Sigmar operator, and the Connor model. For multi-species plasmas, the ambipolar relation, which requires complete cross-species collisional coupling, was confirmed. With the full Hirshman-Sigmar operator, we have confirmed that the widely-used Chang-Hinton analytic model overestimates the ion energy flux in the intermediate aspect ratio regime, by about 22% for our simulation parameters. Agreement with Taguchi's theory, which is the most accurate theoretical result in the banana regime, was demonstrated. The zeroth-order Hirshman-Sigmar operator and the Connor model were found to consistently underestimate the ion energy flux in all collisionality regimes. A study of heavy-ion impurity transport showed that the Hirshman-Sigmar interpolatory theory gives a relatively poor prediction of ion and impurity fluxes. Strong toroidal rotation was found to significantly enhance the impurity fluxes in the banana regime. Extensive studies of rotation effects will be studied in future work.

Finally, parameterized studies of the effects of flux-surface shape (triangularity and elongation) were performed using the Miller local equilibrium model. A simple modification of the Chang-Hinton theory for shaped plasmas which evaluates the magnetic field averages using the exact magnetic field was not found to be generally accurate in predicting the trends of the ion energy flux with shaping paramters. However, it is essential to use the effective magnetic field strength B_{unit} to compute the gyroradius as it occurs in the theory to account for the dominant overall shift due to shaping.

ACKNOWLEDGMENTS

This work was supported by U.S. DOE Grant DE-FG03-95ER54309 and by the Edge Simulation Laboratory project under U.S. DOE Grant DE-FC02-06ER54873.

REFERENCES

1. K.H. Burrell, Phys. Plasmas **4**, 1499 (1997).
2. R.D. Hazeltine, Plasma Phys. **15**, 77 (1973).
3. F.L. Hinton and R.D. Hazeltine, Rev. Mod. Phys. **48**, 239 (1976).
4. S.P. Hirshman and D.J. Sigmar, Nucl. Fusion **21**, 1079 (1981).
5. C.S. Chang and F.L. Hinton, Phys. Fluids **25**, 1493 (1982).
6. S.P. Hirshman, D.J. Sigmar and J.F. Clarke, Phys. Fluids **19**, 656 (1976).
7. S.P. Hirshman and D.J. Sigmar, Phys. Fluids **20**, 418 (1977).
8. F.L. Hinton and S.K. Wong, Phys. Fluids **28**, 3082 (1985).
9. P.J. Catto, I.B. Bernstein and T. Massimo, Phys. Fluids **30**, 2784 (1987).
10. W.A. Houlberg, K.C. Shaing, S.P. Hirshman and M.C. Zarnstorff, Phys. Plasmas **4**, 3230 (1997).
11. E.A. Belli and J. Candy, Plasma Phys. Control. Fusion **50**, 095010 (2008).
12. S.P. Hirshman and D.J. Sigmar, Phys. Fluids **19**, 1532 (1976).
13. J.W. Connor, Plasma Phys. **15**, 765 (1973).
14. L.M. Kovrizhnikh, Report IC/70/86, International Center for Theoretical Physics, Trieste (1970).
15. R.E. Waltz, G.M. Staebler, W. Dorland, G.W. Hammett, M. Kotschenreuther and J.A. Konings, Phys. Plasmas **4**, 2482 (1997).
16. M. Taguchi, Plasma Phys. Control. Fusion **30**, 1897 (1988).
17. O. Sauter, C. Angioni and Y.R. Lin-Liu, Phys. Plasmas **6**, 2834 (1999).
18. G.R. Harris, Report EUR-CEA-FC-1436, Centre détudes de Cadarache, Saint Paul-lez-Durance (1991).
19. R.L. Miller, M.S. Chu, J.M. Greene, Y.R. Lin-Liu and R.E. Waltz, Phys. Plasmas **5**, 973 (1998).
20. R.E. Waltz and R.L. Miller, Phys. Plasmas **6**, 4265 (1999).
21. R.D. Hazeltine, Phys. Fluids **17**, 961 (1974).